Department of Pesticide Regulation
Environmental Monitoring Branch
1001 I Street
Sacramento, California 95814

HYDRUS-simulated flux estimates of 1,3-dichloropropene maximum period-averaged flux and emission ratio for approved application methods

Colin Brown

10/17/2019

Introduction

1,3-Dichloropropene (1,3-D) is a fumigant used to control nematodes, insects and disease organisms in the soil. It is commonly used as a pre-plant treatment that is injected into soil. It may also be applied through drip irrigation. Regardless of the application method, the possibility of offsite transport of this fumigant due to volatilization may subsequently cause human exposure through inhalation. To mitigate its potential cancer risk, the Department of Pesticide Regulation (DPR) limits the use of 1,3-D on a regional basis (township cap). The current township cap is 136,000 “adjusted” pounds during a calendar year in any township (six by six mile area). Adjusted pounds refers to the amount of 1,3-D active ingredient multiplied by an application factor (AF) to account for differences in air concentrations due to application method, region, and season of application.

HYDRUS is a first principles (physics-based) model that uses a finite element method approach to describe movement of heat, water, and solute throughout the soil profile. DPR worked with the developer of HYDRUS to implement a fumigant module that allows for simulation of several applicator practices including tarp cutting and simulation of bedded applications with untarped furrows (see Simunek et al. 2016, Spurlock et al. 2010). Validation work has subsequently shown that the HYDRUS model produces flux estimates comparable to those reported across a range of field studies (Spurlock et al. 2013a, Kandelous 2018), and has additionally indicated that HYDRUS can accurately simulate the fundamental processes of heat, water, and solute transport throughout the soil profile, increasing confidence in the ability of the model to simulate flux under new scenarios (Spurlock et al. 2013a).

DPR has historically relied on estimates of flux reported by a small number of field studies when making regulatory decisions. Whole-field flux cannot be measured directly; therefore, field estimates of flux are estimated from air sampling results--a procedure prone to substantial estimation error (see Majewski 1995). Additionally, the small number of field studies is insufficient to characterize the variability in flux likely to occur for a given application method under a range of environmental conditions, and field flux estimates are not available for a majority of approved application methods. Given the limitations of field studies, HYDRUS simulations are presented here as an alternative method for flux estimation. The capability of HYDRUS to accurately estimate flux across a wide variety of scenarios (including various

combinations of application method, soil type, and environmental conditions) can be applied to establish a lower bound on the variability in flux likely to occur for each method under typical California conditions. HYDRUS may therefore provide more representative flux estimates than can be ordinarily inferred from a small collection of field studies conducted across a limited selection of application methods, soil properties, and environmental conditions.

The objective of this HYDRUS modeling is to simulate post-application volatilization of 1,3-D for 15 out of 17 of the currently-approved application methods for 1,3-D across a range of representative California agricultural soils. The simulations use a data set describing 16 agricultural soils collected by DPR staff in fields prepared for fumigation (i.e., tilled, irrigated). Simulations are performed for every combination of application method and soil type for a total of 240 simulations (15 methods modeled x 16 soils), providing a distribution of flux estimates for each application method. Results include mean, standard deviation for cumulative flux, maximum 24-h flux, and maximum 72-h flux for each of 15 approved 1,3-D application methods. Additionally, differences in cumulative emissions are evaluated over a range of seasonal and regional temperature and evaporation conditions.

Modeling Procedures

All simulations were performed in HYDRUS 2D (v2.04.0580). Flux was assessed by three metrics: maximum 24-h flux based on the maximum rolling average of 1-h time steps ('max 24-h flux', $\mu g\ m^{-2}\ s^{-1}$), max 72-h flux based on the maximum rolling average of 1-h time steps ('max 72-h flux', $\mu g\ m^{-2}\ s^{-1}$), and emission ratio (ER) at 21 days post-application (ER = cumulative flux [$\mu g\ m^{-2}$] / total mass applied [$\mu g\ m^{-2}$]). These metrics were chosen for their use in historical 1,3-D regulation; 24-h and 72-h peak fluxes being used in mitigation of acute exposure, and ER being used in mitigation of lifetime exposure. Details of the HYDRUS model parameterization are described in the sections below.

Application methods

DPR has currently approved 17 field fumigation methods (FFM) for use in 1,3-D applications in California (Table 1), 15 of which were simulated here. The two methods that were not simulated include FFM 1211 ('Nontarpaulin/Deep/GPS-targeted'), a method that encompasses a variety of localized tree-hole type applications in different geometric configurations; and FFM 1290 ('Other label method'), a combined classification for other label-listed application methods. For regulatory purposes, FFM 1211 will be assumed to have the same ER as FFM 1206, the method to which it is most similar, and FFM 1290 will be assumed to share flux characteristics equal to the highest-ER method.

FFMs are typically specific to a certain application geometry (i.e., bedded, broadcast, or strip applications). Field fumigation methods 1201, 1204, and 1206 may be applied to either a bedded or broadcast application. These methods are simulated here as broadcast applications, following evaluation of 2014 Pesticide Use Reporting (PUR) data in which it was suggested that the majority of these applications likely occurred as pre-plant fumigations of the 'broadcast' configuration based on the crop types associated with these application methods (Spurlock 2017, personal communication).

Table 1. List of 1,3-D methods simulated in this study.

Field Fumigation Method (FFM) Code	Method Description
1201	1,3-D - Nontarpaulin/Shallow/Broadcast or Bed
1202	1,3-D – Tarpaulin[1]/Shallow/Broadcast
1203	1,3-D - Tarpaulin/Shallow/Bed
1204	1,3-D - Nontarpaulin/Shallow/Broadcast or Bed w/ 3x Irrigation
1205	1,3-D - Tarpaulin/Shallow/Bed w/ 3x Irrigation
1206	1,3-D - Nontarpaulin/Deep/Broadcast or Bed
1207	1,3-D - Tarpaulin/Deep/Broadcast
1209	1,3-D - Tarpaulin/Chemigation/Bed
1210	1,3-D - Nontarpaulin/Deep/Strip
1242	1,3-D – TIF[2]/Shallow/Broadcast - 60% credit[3]
1243	1,3-D - TIF/Shallow/Bed - 60% credit
1245	1,3-D - TIF/Shallow/Bed w/ 3x Irrigation - 60% credit
1247	1,3-D - TIF/Deep/Broadcast - 60% credit
1249	1,3-D – TIF/Deep/Strip – 60% credit
1259	1,3-D - TIF/Chemigation/Bed - 60% credit

1. Polyethylene (PE) tarp
2. Totally impermeable film
3. '60% credit' refers to a form of buffer zone reduction credit.

Application geometry

Three general formats of application geometry were created to serve as templates for the simulation of each method: broadcast, bedded, and strip (Figure 1). Each field geometry was idealized as a vertical cross-section of a symmetrical application row (also including the inter-row or furrow); half of each row was then simulated for reasons of computational efficiency and domain widths are described in these terms. Dimensions of each field geometry were based on measurements collected by DPR of representative field types. Broadcast domain width was set to 183 cm based on geometry of a single pass in a typical field fumigation with tarp (Spurlock 2015a). Strip domain width was set to 251 cm based on common application geometry in orchards, where strip applications are typically used (Spurlock 2014). Bedded domain width was set to 60 cm with a bed width of 32.5 cm based on field measurements of typical strawberry beds in Monterey County taken as part of an unpublished drip study (Spurlock 2016). Domain depth was set to 120 cm for all application types based on prior observations that domain depths of > 100 cm have essentially no effect on ER or maximum flux (Spurlock 2016).

A given application geometry was paired with one of three application depths as required by the method being simulated: surface chemigation, shallow shank injection, or deep shank injection. Depth of application for shank applications was based on the minimum regulatory application depth, whereas injection spacing was based on measurements of fumigation rigs collected during DPR observation of

field fumigations. Surface chemigation was simulated by placement of a drip line centered 5 cm below the soil surface and emitting uniformly around the circumference of the line. Broadcast and bedded shank injections were simulated by placement of an initial plug of solute centered 30 cm or 45 cm below the soil surface for shallow and deep applications, respectively. Broadcast shank injection solute plugs measured 10 cm high by 80 cm wide with two plugs per row. Bedded shank injection plugs measured 10 cm by 10 cm with two plugs per row. Strip applications utilized solute plugs measuring 10 cm by 10 cm with seven plugs per row. Keeping in line with DPR conventions, concentrations in each simulation were based on a 100 lb/ac application rate to allow for comparison across methods.

Tarping (polyethylene [PE] tarp and totally impermeable film [TIF]) was simulated with increased resistance at the soil surface. Broadcast tarped applications employed a continuous layer of tarp over the soil surface across the entirety of the simulation domain, whereas bedded and strip tarped applications were simulated with a discontinuous coverage at the soil surface (i.e., untarped furrows). Additional details regarding the parameterization of the surface boundary are described in later sections.

The bottom boundary conditions in every simulation were set to "free drainage" for water flow and "third-type" boundary conditions for solute transport and heat transport. No water flow, solute transport, or heat transport was allowed to occur through the sides of the simulation domain.

Table A-1 (Appendix A) summarizes the combination of application geometry, depth, tarping method, and other factors used to describe each FFM for modeling purposes.

Application Timing

The simulation time domain for shank methods began immediately following completion of fumigation (i.e., immediately following application of the fumigant to the soil), assumed to be 8:00 am on the day of application. Simulations for chemigation methods began at the start of the application period, assumed to be 8:00 am, beginning with a 20-minute pre-application irrigation of fresh water as recommended by product labeling. Application of fumigant through the drip line began at 8:20 am on the day of application and continued for 4 h. Chemigation applications were completed with a 20-minute flushing of the drip line with fresh water as required by regulation (3 CCR 6448.1[d]).

In the case of methods requiring a series of post-fumigation water seals (FFM codes 1204, 1205, and 1245), irrigation was applied at a rate of 0.30-0.64 cm/h (0.15-0.25 in/h) in total volumes corresponding to the minimum requirement according to soil texture class (Table 2) as specified in regulation (3 CCR 6448.1[d]), which specifies:

> *(b) Fumigation methods using post-water treatments must be applied at a rate of 0.15-0.25 inches per hour and meet one of the following water requirements depending on soil texture:*
> *(1) coarse soils - a minimum of 0.40 inches of water per acre.*
> *(2) loamy, moderately coarse, or medium texture soils - a minimum of 0.30 inches of water per acre.*
> *(3) fine texture soils - a minimum of 0.20 inches of water per acre.*

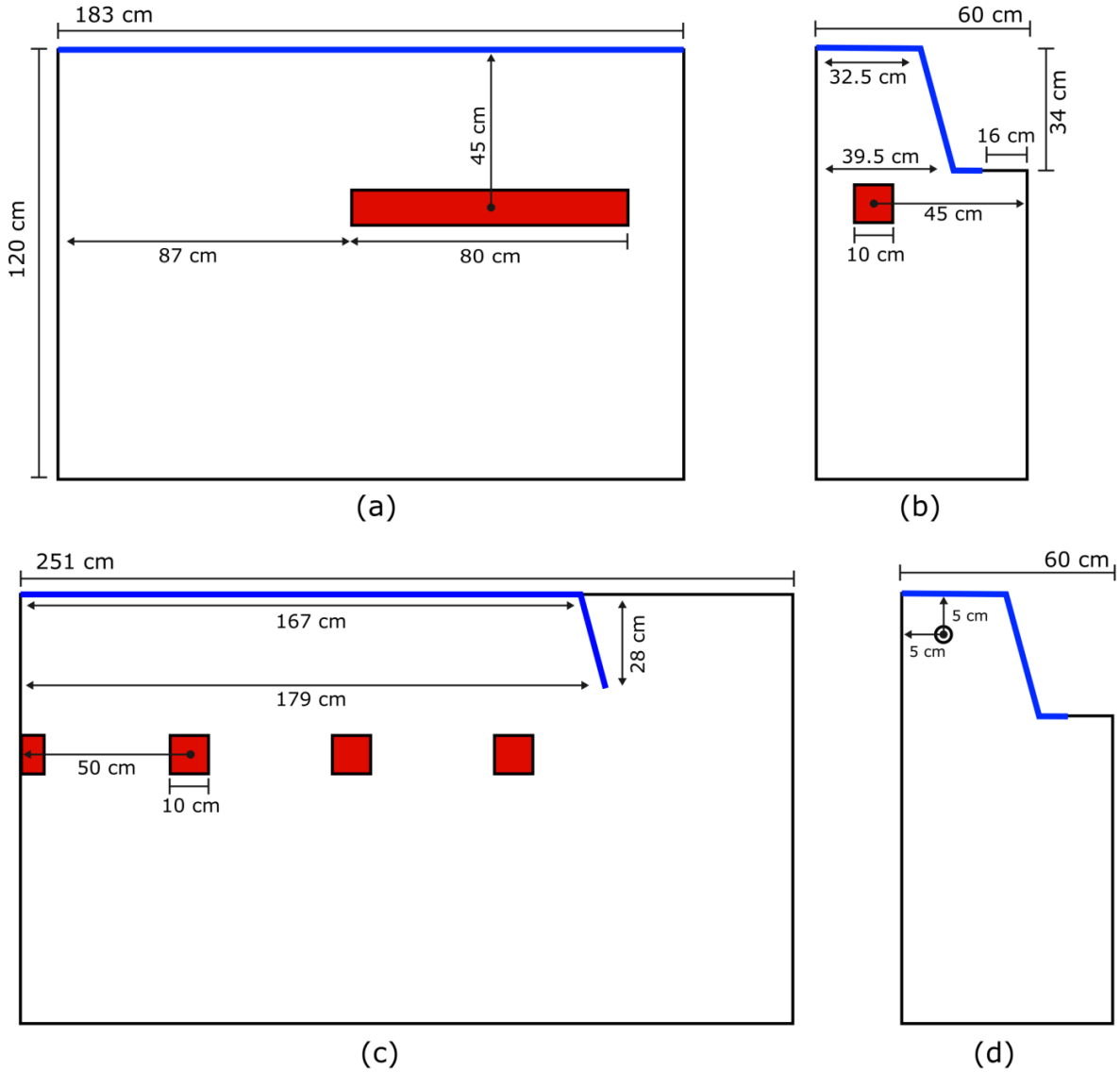

Figure 1. Examples of domain geometries used in simulating fumigation methods in HYDRUS. The initial solute distribution and surface tarp configuration are displayed for hypothetical scenarios: (a) deep shank broadcast fumigation under tarp; (b) deep shank bedded fumigation under tarp; (c) deep shank strip fumigation under tarp; and (d) bedded chemigation under tarp. Initial solute plugs are displayed in red for shank applications, whereas solute enters the domain from a simulated drip line towards the top left of the chemigation domain geometry. Simulated tarp is indicated in blue.

Table 2. Label texture categories and their relation to USDA soil texture classes. Texture categories are used to determine the volume of water applied for post-application irrigation water treatments.

Texture Category	USDA Texture Classes
Coarse soils	Fine sand, loamy fine sand
Moderately coarse soils	Sandy loam, fine sandy loam
Medium textured soils	Sandy clay loam, loam, silt loam
Fine textured soils	Clay, clay loam, silty clay loam

In the event that a post-fumigation sprinkler irrigation occurred over a tarped bed, it was assumed that all water would run off the tarped bed and into the uncovered furrows.

A simulated tarp cutting was included at 5 or 9 days following the end of the application, depending on tarp type being simulated (PE or TIF, respectively). 'End of application' was considered as 8:00 am on the day of application for shank applications, and either 12:00 pm or 4:30 pm on the day of application for high-flow and low-flow chemigation applications, respectively. Following tarp cutting, the resistance at the soil surface was decreased to the value of bare soil (d = 0.5).

Soil data

Soil core data were collected by DPR staff from 16 different fields prepared for field fumigation. Four to 12 cores were collected in each field, and averaged core data was used to represent each soil parameter at a given sampling depth. Soil cores were typically retrieved from depths of 0-10 cm, 10-30 cm, and 30-50 cm. Three fields sampled in Lost Hills, California, were retrieved from depths of 0-20 cm, 20-40 cm, 40-60 cm, and 60-80 cm and one field sampled in 2017 near Castroville, California, was sampled in 10-cm increments from 0-50 cm depth. All soil cores were analyzed for bulk density, volumetric water content, and sand, silt, and clay percentages (soil texture analysis). Soil porosity was calculated from bulk density with an assumed particle density of 2.65 g/cm^3. Soil organic carbon was measured at three fields in Lost Hills. Table A-2 (Appendix A) summarizes soils data.

Within HYDRUS, measured soil properties were used to describe soil properties at three depth categories of 0-10 cm, 10-30 cm, and 30-120 cm. The soil core sampling depth of measured soil properties were assigned to the nearest matching depth category in HYDRUS; in the majority of cases, soil cores obtained from depths of 0-10 cm, 10-30 cm, and 30-50 cm were used to represent soil properties at depths of 0-10 cm, 10-30 cm, and 30-120 cm in HYDRUS. For Castroville soils data, averages of soil core data collected at 10-20 cm and 20-30 cm were used to represent the 10-30 cm depth in HYDRUS, and averages of 30-40 cm and 40-50 cm soil core data were used to represent the 30-120 cm depth in HYDRUS. Lost Hills soils data from 0-20 cm, 20-40 cm, and 40-60 cm were applied to represent soil properties at 0-10 cm, 10-30 cm, and 30-120 cm, respectively.

HYDRUS requires specification of several fitted soil hydraulic parameters for input into the model's soil-water retention function. While these parameters may be fitted directly to measured soil-water retention data for each soil, the necessary laboratory procedures are extremely challenging and are subject to unknown amounts of error, particularly when attempting to characterize an entire agricultural field. Here, we rely upon the HYDRUS implementation of the ROSETTA pedotransfer functions, a well-vetted and widely used model that uses easy-to-measure input variables (bulk density, soil texture) to estimate soil water retention and hydraulic conductivity curve parameters from experimental data for 2000+ soils (Schaap et al. 2001).

Modeling parameters

Fumigant physicochemical properties were those used in previous HYDRUS modeling studies, including Spurlock et al. (2013a), and are summarized in Tables A-3 and A-4. The fumigant organic carbon-normalized soil sorption coefficient K_{OC} and the 1,3-D degradation rate constant k_1 are optimized values from calibration of HYDRUS to field flux estimates (Spurlock et al. 2013a). These variables have a substantial influence on simulated flux and are difficult to measure directly (Spurlock et al. 2013b).

Tarp permeability was simulated by varying the resistance at the soil surface (*d*). The value of *d* for PE tarp was calculated based on the mean value of laboratory-estimated mass transfer coefficients. Laboratory-measured and field-estimated mass transfer coefficients for TIF tarp have been found to differ by several orders of magnitude (Spurlock et al. 2013a), possibly due to changes in the tarp behavior under field conditions resulting from weathering (Ajwa 2008, via Johnson and Spurlock 2012), as well as the tearing, stretching, and gluing of seams that occur under field conditions (Qin et al. 2011). Therefore, we use calibrated field-effective *d* values for TIF tarp (Spurlock et al. 2013a).

Diurnal variation in soil surface temperature (SST) and evaporation for untarped fumigations were estimated based on the model described by Spurlock (2013) using maximum and minimum air temperature values and average daily evapotranspiration values for the month of September between 2012-2016 as obtained from California Irrigation Management Information System (CIMIS) Station #2 at Five Points, located in Fresno County (CIMIS 2018). The potential evaporative water flux was set to zero for tarped portions of each modeling domain. Daily potential evaporation of 0.57 cm was used for the untarped portion of the soil surface based on reference evapotranspiration rates in Fresno County under September conditions. A matric potential of -15,000 cm was used as the limiting soil surface pressure head, below which actual evaporation is less than potential evaporation (i.e., soil-limited evaporation). Soil surface temperature for PE-tarped applications used the same SST model as above, using below-tarp soil temperature data obtained from Yates et al. (1996) via Spurlock (2013) to estimate the difference between air temperature and SST under the PE tarp. Zero evaporation was assumed to occur through tarped surfaces.

Soil surface temperature for TIF methods was parameterized using actual below-tarp SST measured by DPR's Air Program (Spurlock et al. 2013c, Tuli 2011) during a June 2011 field fumigation study in Kern County (Ajwa and Sullivan 2012). That temperature data was collected on a surrogate field that was treated identically to the fumigated fields apart from the application of fumigant (Spurlock et al. 2013a).

Regional and Seasonal Temperature Variation

The effect of seasonal and regional temperature variation on cumulative flux was evaluated by simulating FFM 1206 (Nontarpaulin/Deep/Broadcast) across 16 soils types for each of 6 locations and 2 seasons. The selected locations consisted of three coastal and three inland regions throughout California (Figure 2), each associated with relatively high historical 1,3-D use. Temperature and evaporation conditions at each location were retrieved for the summer and winter seasons, here defined as September and January, respectively, based on timing of maximum and minimum annual mean air temperature, as well as corresponding to the timing of peak 1,3-D application periods. Ambient air temperature and evaporation data were retrieved from CIMIS stations at 5 out of 6 locations; CIMIS data was not available in Del Norte County; air temperature data was instead retrieved from the Automated Surface Observing System meteorological station at Crescent City airport with daily total evaporation from Salinas assumed as representative.

Table 3 summarizes mean maximum daily air temperature and mean minimum daily air temperature by location and season. Diurnal variation in SST and evaporation was estimated using the model described by Spurlock (2013). The difference between air temperature and SST was assumed constant across all scenarios.

Table 3. Summary of air temperature values by site and soil temperature delta values used to estimate soil surface temperature variability using the model from Spurlock (2013).

County	September [warm]		January [cool]		Soil Temperature	
	Max Air Temp [°C]	Min Air Temp [°C]	Max Air Temp [°C]	Min Air Temp [°C]	Soil Max ΔT [°C]	Soil Min ΔT [°C]
Del Norte	16.80	10.70	12.70	5.60	11.0	1.0
Monterey	20.72	11.25	16.20	5.56		
Ventura	26.00	12.93	20.51	7.50		
Merced	31.75	12.86	14.41	0.99		
Fresno	31.80	14.39	14.44	2.85		
Imperial	36.89	21.06	20.76	2.94		

A season-location interaction on cumulative flux was evaluated using a two-way repeated measures ANOVA in R (version 3.4.2), whereby each soil type was considered an independent subject over which a treatment of location and season was applied. Cumulative flux was evaluated at 30 days post-application to take into account the longer period of emissions under cool conditions. The objective of the approach is to identify whether a significant seasonal or regional temperature effect exists that should be accounted for when estimating ER for regulatory purposes.

Post-processing

HYDRUS output of 1-h discrete period-averaged flux was converted to units of ug m^{-2} s^{-1}. Max 24-h flux and max 72-h flux for each simulation was then identified via rolling average of 1-h time steps. Method ER was calculated as the ratio of the cumulative flux value at a given time step to the total mass of

fumigant applied. Emission ratio is reported at 21 days for all methods. Standard deviation (SD) was calculated for each quantity as a measure of the variability around the mean.

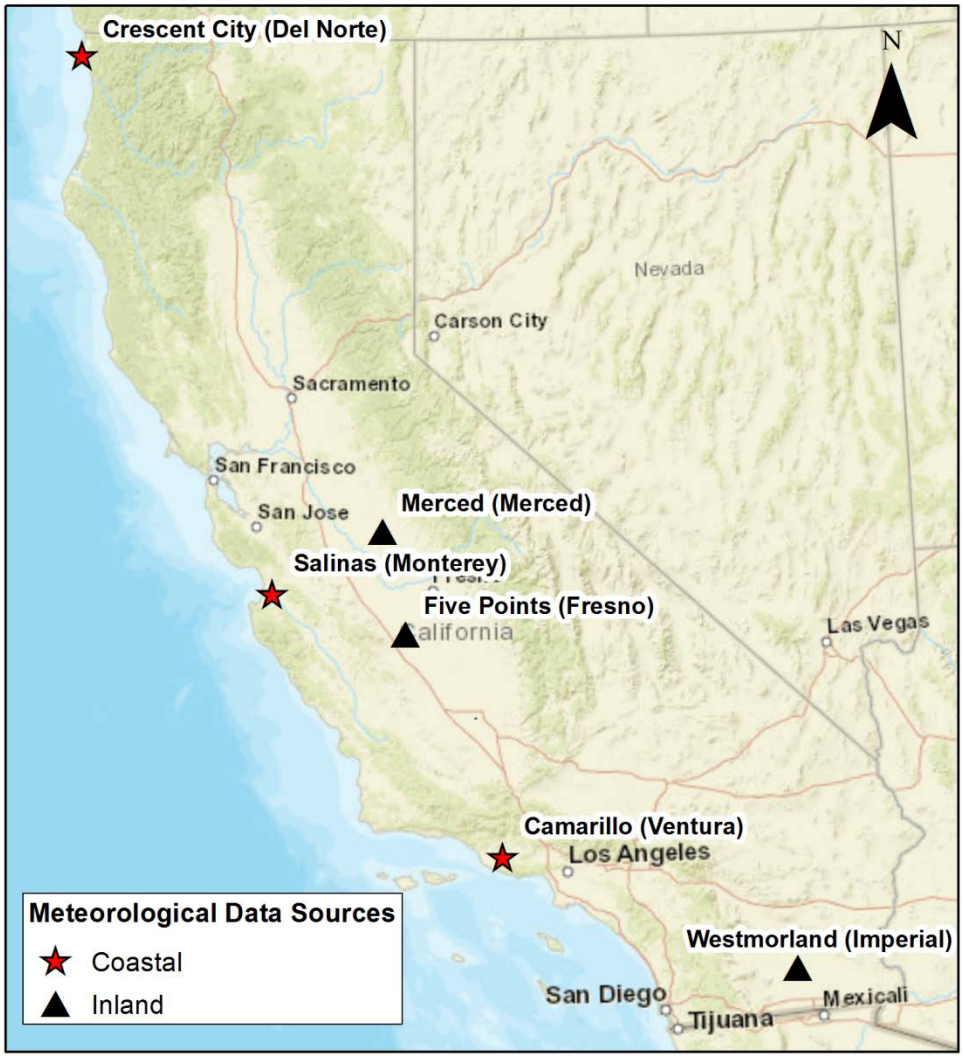

Figure 2. Meteorological data sources from which air temperature and evaporation data were retrieved for the purposes of evaluating seasonal and regional differences in cumulative flux by season and region. Evaporation data was not available from the meteorological station in Del Norte County; Salinas evaporation rates were assumed.

Results and Discussion

Flux Estimates

Table 4 summarizes max 24-h flux, max 72-h flux, and ER at 21 days post-application from HYDRUS simulation output. Standard deviation is provided as a measure of variability around the mean of each value resulting from variation across the 16 soil types simulated. Quantile-comparison plots indicated that the distribution of maximum flux and ER values were approximately normal within method. Max

24-h flux, max 72-h flux, and ER were strongly correlated across methods. Across simulations, mean ER varied from a minimum of 0.11 ± 0.05 (FFM 1247 [TIF/Deep/Broadcast]) to a maximum of 0.58 ± 0.09 (FFM 1201 [Nontarpaulin/Shallow/Broadcast]). Mean max 24-h flux varied from a minimum of 2.93 ± 0.98 μg m^{-2} s^{-1} (FFM 1242 [TIF/Shallow/Broadcast]) to a maximum of 32.40 ± 12.11 μg m^{-2} s^{-1} (FFM 1201). Mean max 72-h flux varied from a minimum of 1.61 ± 0.71 μg m^{-2} s^{-1} (FFM 1247) to a maximum of 19.59 ± 4.68 μg m^{-2} s^{-1} (FFM 1201).

Coefficient of variation (CV = SD / mean) describes the percent variation of 1 SD around the mean for a given method (i.e., the range of values expected to contain 68% of observations in normally-distributed data.) Here, CV describes variation in flux due to variation in soil properties. Coefficient of variation for max 24-h flux varied from 23% to 67%. Coefficient of variation for max 72-h flux varied from 21% to 57%. Coefficient of variation for ER varied from 15% to 53%. In general, deep shank applications were the most variable and chemigation applications the least variable. Increased variability with depth may relate to the increased interaction between fumigant and soil properties due to the increased path length from the injection point to the soil surface. In the specific case of chemigation, use of irrigation water raises soil water content in the region around the emitter to field capacity and thus minimizes variation relating to initial soil water content across the 16 soil types.

Table 5 presents detailed results for each combination of method and soil type. Tables B-1 and B-2 (Appendix B) provide raw simulation output of HYDRUS cumulative flux and 1-h period average flux.

End-of-simulation fumigant mass balance error as a percentage of fumigant applied was within the acceptable range; all were less than 1.54%, indicating very low numerical error.

Soil Organic Carbon

The sensitivity analysis performed by Spurlock et al. (2013b) evaluated the effects of soil parameters including soil water content, saturated soil water content, bulk density, and soil organic carbon (SOC). DPR soil sampling included measurement of the first three of these parameters for all fields, whereas SOC measurements were only taken in three fields. Soil organic carbon, evaluated in Spurlock et al. (2013b) as the soil-water partitioning coefficient Kd (= Koc * SOC), is a moderate-to-high-sensitivity parameter in the determination flux output, approximately equivalent (and having a similar computational role) to bulk density in terms of model sensitivity, and increasing percent SOC will act to slow solute transport due to increased soil sorption. Spurlock (2016) evaluated the utility of the Soil Survey Geographic Data Base (SSURGO) as a reference for SOC or organic matter distributions and noted a great deal of uncertainty due to variation in analysis methods and a lack of clarity in whether samples were retrieved from undisturbed soils or cultivated agricultural lands. For that reason, modeling here uses actual SOC data from fumigated fields. Additional work to characterize SOC in fumigated fields would be a useful complement to future modeling efforts.

Influence of Seasonal and Regional Temperature Variation

Minor but significant differences in cumulative flux were estimated in response to interactions between seasonal and regional temperature variation when controlling for soil type. Mean (M) and standard

error (SE) of effect size were contrasted to the mean of each level. All main effects and interactions were significant at least p = 0.01, indicating a significant difference in cumulative flux on the basis of region (M = 141, SE = 100), season (M = 682, SE = 195), and region:season interaction (M = 117, SE = 144). The significant interaction effect suggests that the strength of a seasonal effect on cumulative flux will vary by region. Differences in group means of up to 4% were observed, with cooler conditions resulting in slightly higher cumulative flux than warmer conditions (Figure 3). However, variance due to location and season were greatly outweighed by variance due to soil properties, and some dry soils were observed to produce higher emissions under warm rather than cool conditions. Given that the distribution of soil properties is not constant across time and space, the overall result suggests that temperature effects on cumulative flux are likely to be minor in comparison to regional or seasonal variation in soil moisture and soil properties. Some of these soil conditions are fixed by location (i.e., regional variation in soil type), but key variables such as soil moisture (to which flux is sensitive) will depend on the practices of individual growers. Group means were not significantly different when soil type was not included as an explanatory variable (p = 0.89).

The conclusion of this assessment runs somewhat contrary to the prior assumption by which cumulative flux has been thought to be greater under warm conditions (e.g., the extrapolation of summertime ERs from cool season flux field studies described by Johnson 2013). This assumption may have followed from the observation of higher peak fluxes under warm conditions, and field study durations of typically less than 2 weeks. Under the modeled scenarios, cumulative flux under warm conditions generally does not exceed that of cool conditions within the first 2 weeks post-application, but an extended period of flux occurring under cool conditions ultimately results in higher cumulative flux values at 30 days (720 h) post-application in a majority of soils. The underlying physicochemical mechanism appears to be an interaction between temperature, 1,3-D degradation rate, and diffusion coefficients. Under cool conditions, slowed diffusion rates and increased partitioning of 1,3-D into the aqueous phase result in lower peak fluxes and lower cumulative fluxes in the short-term. However, slowed degradation rate extends the volatilization period to produce higher cumulative fluxes in the long-term in a majority of soils evaluated (Figure 4). The possibility of this interaction was previously described by Spurlock (2016), who noted a lack of studies demonstrating the effect of low temperatures on fumigant field flux.

Table 4. Estimates (mean values) of max 24-h flux, max 72-h flux, and emission ratio (ER) at 21 days post-application obtained from HYDRUS simulations of each method performed across a dataset of 16 different soil types. Standard deviation (SD) is provided for each estimate as a measure of the variability associated with each method due to variation in soil characteristics.

FFM code	Method description	Max 24-h flux* ($\mu g\ m^{-2}\ s^{-1}$)	SD ($\mu g\ m^{-2}\ s^{-1}$)	Max 72-h flux* ($\mu g\ m^{-2}\ s^{-1}$)	SD ($\mu g\ m^{-2}\ s^{-1}$)	ER @ 21 days	SD
1201	1,3-D - Nontarpaulin/Shallow/Broadcast	32.40	12.11	19.59	4.68	0.58	0.09
1202	1,3-D - Tarpaulin/Shallow/Broadcast	23.00	9.45	14.82	4.76	0.46	0.12
1203	1,3-D - Tarpaulin/Shallow/Bed	30.46	11.44	19.05	5.37	0.55	0.11
1204	1,3-D - Nontarpaulin/Shallow/Broadcast w/ 3x Irrigation	24.60	10.53	15.70	4.96	0.50	0.10
1205	1,3-D - Tarpaulin/Shallow/Bed w/ 3x Irrigation	28.49	10.29	17.72	4.85	0.52	0.11
1206	1,3-D - Nontarpaulin/Deep/Broadcast	13.63	8.46	10.17	4.99	0.38	0.13
1207	1,3-D - Tarpaulin/Deep/Broadcast	9.89	6.62	7.80	4.46	0.31	0.14
1209	1,3-D - Tarpaulin/Chemigation/Bed	30.46	6.87	16.85	3.50	0.48	0.08
1210	1,3-D - Nontarpaulin/Deep/Strip	12.73	8.31	9.75	5.07	0.39	0.14
1242	1,3-D - TIF/Shallow/Broadcast - 60% credit	2.93	0.98	2.66	0.82	0.14	0.05
1243	1,3-D - TIF/Shallow/Bed - 60% credit	7.16	3.65	6.33	2.95	0.26	0.10
1245	1,3-D - TIF/Shallow/Bed w/ 3x irrigation - 60% credit	4.81	1.74	4.37	1.46	0.20	0.06
1247	1,3-D - TIF/Deep/Broadcast - 60% credit	3.07	1.41	1.61	0.71	0.11	0.05
1249	1,3-D - TIF/Deep/Strip - 60% credit	3.11	1.29	2.06	1.05	0.14	0.07
1259	1,3-D - TIF/Chemigation/Bed - 60% credit	5.94	2.15	5.12	1.83	0.20	0.06

* Reported on a 100 lb/ac basis.

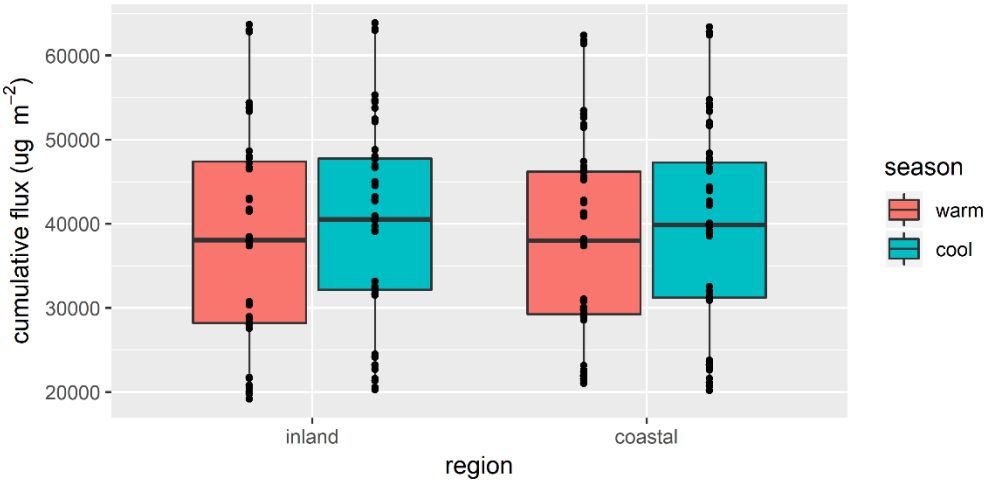

Figure 3. Distribution of HYDRUS cumulative flux estimates by season and region. Boxes span the interquartile range (middle 50% of flux estimates) and the median value is indicated by the horizontal bar. Whiskers span the range of maximum and minimum flux estimates. Bolded points represent the value of individual simulations.

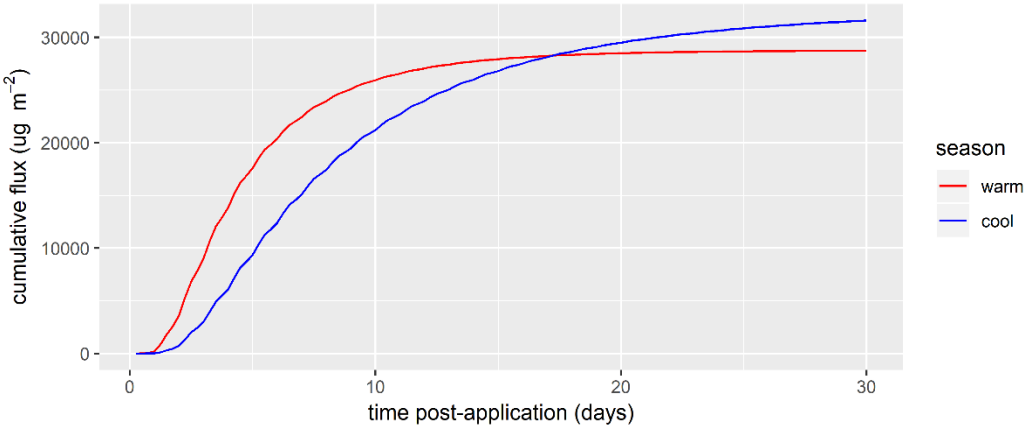

Figure 4. Example of simulated cumulative flux time series under both warm and cool conditions for FFM 1206, soil #1 (loam) under Fresno temperature conditions. Cumulative flux is reported at 6-h intervals to 30 days post-application. Lower initial cumulative fluxes in cool soils will typically exceed those in warm soils given a period of two or more weeks following application. In the scenario above, cumulative flux under cool conditions exceeds that of warm conditions approximately 17 days post-application.

A notable limitation of the approach taken to evaluate seasonal and regional influences is the method by which SST is parameterized under each treatment. The relationship between SST and air temperature is not well understood, and here relies on measurements from a small collection of field studies. It is likely that the relationship between air temperature and soil temperature varies somewhat by season and location, introducing a source of uncertainty in the comparison. The publication of high-quality SST

data, paired with on-site ambient air temperature data, could reduce some of the uncertainty associated with the current approach. For bare soil SST specifically, a direction of future research could include the evaluation of remotely sensed radiometer data to refine SST estimates across a variety of seasons and locations.

As is the case for simplified SST estimates, limitations in the soils dataset necessitate soil parameter distributions (including soil moisture and soil texture) that are assumed constant across regions, whereas substantial regional variation can be expected under real world conditions (see Johnson and Spurlock 2009 for an evaluation of the soil types associated with 1,3-D applications in certain regions of California). While there may be real differences in mean fluxes that occur due to regional or seasonal differences in soil conditions, such in-depth analysis is not currently possible due to data limitations.

Table 5. Summary of individual simulation results for HYDRUS-estimated max 24-h flux, max 72-h flux, and emission ratio (ER).

FFM code	Max 24-h flux* ($\mu g\ m^{-2}\ s^{-1}$)	Max 72-h flux* ($\mu g\ m^{-2}\ s^{-1}$)	ER @ 21 d	Soil no.
1201	21.11	15.29	0.50	1
1201	15.42	12.67	0.46	2
1201	14.54	11.86	0.44	3
1201	45.02	24.47	0.67	4
1201	56.25	27.47	0.75	5
1201	45.40	24.36	0.68	6
1201	30.13	19.17	0.57	7
1201	39.92	22.85	0.64	8
1201	43.95	23.91	0.67	9
1201	23.76	16.78	0.54	10
1201	31.92	19.48	0.58	11
1201	22.10	14.99	0.49	12
1201	41.01	23.57	0.65	13
1201	22.32	15.82	0.52	14
1201	35.58	21.74	0.63	15
1201	29.96	19.00	0.57	16
1202	14.38	10.76	0.36	1
1202	7.01	5.90	0.23	2
1202	7.37	6.17	0.24	3
1202	32.29	19.46	0.56	4
1202	41.46	23.14	0.67	5
1202	34.40	20.16	0.58	6
1202	21.96	14.53	0.45	7
1202	28.37	17.64	0.52	8
1202	26.73	16.69	0.51	9

FFM code	Max 24-h flux* ($\mu g\ m^{-2}\ s^{-1}$)	Max 72-h flux* ($\mu g\ m^{-2}\ s^{-1}$)	ER @ 21 d	Soil no.
1202	16.16	11.87	0.39	10
1202	24.84	15.88	0.48	11
1202	17.86	12.48	0.41	12
1202	30.04	18.63	0.54	13
1202	17.53	12.54	0.41	14
1202	25.76	16.67	0.50	15
1202	21.87	14.53	0.45	16
1203	23.57	16.06	0.49	1
1203	13.36	10.26	0.36	2
1203	12.95	10.08	0.35	3
1203	42.26	24.27	0.65	4
1203	54.17	29.33	0.77	5
1203	46.43	25.98	0.69	6
1203	33.86	20.82	0.58	7
1203	32.78	20.74	0.59	8
1203	28.39	19.01	0.57	9
1203	21.59	15.20	0.48	10
1203	37.74	22.68	0.62	11
1203	18.47	12.89	0.42	12
1203	36.14	21.89	0.60	13
1203	24.92	16.91	0.51	14
1203	30.71	19.48	0.55	15
1203	29.96	19.23	0.56	16
1204	13.57	10.84	0.41	1
1204	7.05	6.40	0.31	2
1204	7.20	6.52	0.31	3
1204	38.94	21.90	0.61	4
1204	41.46	22.40	0.65	5
1204	34.34	19.83	0.58	6
1204	23.83	15.91	0.50	7
1204	32.30	19.59	0.57	8
1204	33.05	19.79	0.58	9
1204	18.39	13.76	0.46	10
1204	25.04	15.98	0.50	11
1204	16.70	12.07	0.42	12
1204	32.47	19.64	0.57	13
1204	17.76	12.98	0.45	14
1204	26.61	17.29	0.53	15
1204	24.86	16.32	0.50	16
1205	22.20	14.92	0.46	1
1205	12.35	9.28	0.33	2

FFM code	Max 24-h flux* (μg m^{-2} s^{-1})	Max 72-h flux* (μg m^{-2} s^{-1})	ER @ 21 d	Soil no.
1205	12.01	9.18	0.33	3
1205	40.36	23.05	0.63	4
1205	48.55	26.43	0.72	5
1205	41.96	23.43	0.64	6
1205	32.16	19.53	0.55	7
1205	30.56	19.26	0.56	8
1205	24.93	16.77	0.52	9
1205	20.90	14.62	0.46	10
1205	34.56	20.66	0.58	11
1205	18.26	12.69	0.41	12
1205	35.01	20.99	0.58	13
1205	24.18	16.24	0.50	14
1205	29.54	18.50	0.53	15
1205	28.26	18.00	0.53	16
1206	7.09	6.30	0.29	1
1206	4.16	3.91	0.22	2
1206	3.93	3.68	0.20	3
1206	19.56	14.01	0.48	4
1206	32.59	19.86	0.63	5
1206	24.54	16.47	0.54	6
1206	11.60	9.62	0.38	7
1206	18.31	13.43	0.47	8
1206	24.14	16.26	0.54	9
1206	7.71	6.79	0.31	10
1206	15.37	11.87	0.43	11
1206	3.75	3.53	0.20	12
1206	14.77	11.51	0.42	13
1206	6.25	5.70	0.28	14
1206	11.92	9.81	0.38	15
1206	12.36	9.97	0.38	16
1207	4.78	4.36	0.21	1
1207	1.52	1.35	0.09	2
1207	1.76	1.58	0.10	3
1207	14.21	11.28	0.42	4
1207	25.26	16.89	0.58	5
1207	19.57	13.98	0.48	6
1207	8.67	7.28	0.30	7
1207	13.26	10.57	0.39	8
1207	15.48	11.59	0.42	9
1207	5.05	4.64	0.23	10
1207	12.40	9.99	0.38	11

FFM code	Max 24-h flux* ($\mu g\ m^{-2}\ s^{-1}$)	Max 72-h flux* ($\mu g\ m^{-2}\ s^{-1}$)	ER @ 21 d	Soil no.
1207	3.12	2.96	0.17	12
1207	10.67	8.89	0.35	13
1207	4.92	4.55	0.22	14
1207	8.50	7.23	0.31	15
1207	9.11	7.66	0.32	16
1209	23.61	14.14	0.43	1
1209	19.52	11.01	0.35	2
1209	18.21	10.65	0.33	3
1209	35.76	19.74	0.55	4
1209	42.88	23.92	0.64	5
1209	36.04	21.09	0.58	6
1209	31.08	17.48	0.49	7
1209	34.54	18.24	0.52	8
1209	40.08	20.03	0.56	9
1209	24.31	14.16	0.44	10
1209	30.62	17.33	0.50	11
1209	27.95	15.02	0.43	12
1209	31.77	17.48	0.51	13
1209	27.00	14.91	0.44	14
1209	33.72	17.48	0.49	15
1209	30.24	16.88	0.49	16
1210	6.62	5.99	0.29	1
1210	3.92	3.70	0.22	2
1210	3.59	3.40	0.20	3
1210	17.70	13.39	0.48	4
1210	31.94	19.84	0.65	5
1210	23.90	16.38	0.56	6
1210	10.96	9.27	0.38	7
1210	17.05	13.00	0.47	8
1210	23.08	16.10	0.55	9
1210	6.85	6.20	0.30	10
1210	15.10	11.77	0.44	11
1210	3.10	2.94	0.19	12
1210	12.62	10.43	0.41	13
1210	5.74	5.30	0.28	14
1210	10.19	8.79	0.38	15
1210	11.34	9.48	0.38	16
1242	2.25	2.02	0.11	1
1242	1.59	1.35	0.07	2
1242	1.64	1.40	0.08	3
1242	3.50	3.27	0.18	4

FFM code	Max 24-h flux* ($\mu g\ m^{-2}\ s^{-1}$)	Max 72-h flux* ($\mu g\ m^{-2}\ s^{-1}$)	ER @ 21 d	Soil no.
1242	5.75	4.59	0.27	5
1242	3.95	3.73	0.20	6
1242	2.64	2.43	0.13	7
1242	3.16	3.00	0.16	8
1242	2.90	2.76	0.15	9
1242	2.45	2.23	0.12	10
1242	3.05	2.82	0.15	11
1242	2.51	2.32	0.12	12
1242	3.37	3.19	0.16	13
1242	2.57	2.34	0.12	14
1242	3.01	2.81	0.14	15
1242	2.53	2.35	0.13	16
1243	5.14	4.68	0.20	1
1243	3.02	2.71	0.12	2
1243	3.07	2.75	0.13	3
1243	8.97	8.00	0.32	4
1243	15.67	12.73	0.50	5
1243	12.74	10.55	0.40	6
1243	7.29	6.76	0.27	7
1243	7.99	7.41	0.30	8
1243	9.84	8.66	0.35	9
1243	4.62	4.19	0.19	10
1243	10.27	8.94	0.34	11
1243	2.58	2.38	0.12	12
1243	6.44	6.02	0.24	13
1243	4.61	4.23	0.19	14
1243	5.37	4.95	0.21	15
1243	6.86	6.39	0.26	16
1245	3.84	3.46	0.16	1
1245	2.43	2.21	0.11	2
1245	2.48	2.22	0.11	3
1245	6.12	5.51	0.25	4
1245	8.56	7.07	0.34	5
1245	7.10	5.98	0.26	6
1245	5.40	4.93	0.21	7
1245	5.15	5.05	0.24	8
1245	5.92	5.78	0.27	9
1245	3.73	3.44	0.16	10
1245	6.40	5.68	0.24	11
1245	2.54	2.34	0.12	12
1245	4.84	4.43	0.19	13

FFM code	Max 24-h flux* ($\mu g\ m^{-2}\ s^{-1}$)	Max 72-h flux* ($\mu g\ m^{-2}\ s^{-1}$)	ER @ 21 d	Soil no.
1245	3.78	3.52	0.17	14
1245	4.17	3.79	0.17	15
1245	4.55	4.43	0.21	16
1247	2.21	1.11	0.07	1
1247	1.23	0.67	0.04	2
1247	1.36	0.73	0.04	3
1247	4.06	2.03	0.14	4
1247	7.21	3.46	0.26	5
1247	4.43	2.62	0.17	6
1247	2.58	1.37	0.09	7
1247	3.30	1.91	0.13	8
1247	3.55	1.95	0.14	9
1247	2.61	1.30	0.08	10
1247	3.24	1.90	0.13	11
1247	1.96	1.00	0.06	12
1247	3.29	1.68	0.11	13
1247	2.45	1.24	0.08	14
1247	2.67	1.40	0.10	15
1247	2.91	1.45	0.10	16
1249	2.32	1.27	0.09	1
1249	1.29	0.79	0.05	2
1249	1.41	0.84	0.05	3
1249	4.15	2.64	0.18	4
1249	6.78	4.75	0.33	5
1249	4.27	3.53	0.22	6
1249	2.70	1.72	0.12	7
1249	3.39	2.51	0.17	8
1249	3.57	2.91	0.19	9
1249	2.76	1.50	0.10	10
1249	3.26	2.46	0.16	11
1249	2.00	1.12	0.07	12
1249	3.39	2.03	0.14	13
1249	2.59	1.44	0.09	14
1249	2.80	1.66	0.12	15
1249	3.07	1.76	0.13	16
1259	4.30	3.81	0.16	1
1259	3.69	3.07	0.12	2
1259	3.83	3.18	0.13	3
1259	6.81	6.10	0.24	4
1259	11.93	9.88	0.36	5
1259	9.62	8.28	0.31	6

FFM code	Max 24-h flux* ($\mu g\ m^{-2}\ s^{-1}$)	Max 72-h flux* ($\mu g\ m^{-2}\ s^{-1}$)	ER @ 21 d	Soil no.
1259	5.18	4.77	0.19	7
1259	6.30	5.52	0.22	8
1259	6.32	5.56	0.23	9
1259	4.56	3.81	0.16	10
1259	6.86	6.18	0.24	11
1259	5.17	3.95	0.14	12
1259	5.42	4.77	0.19	13
1259	4.69	3.89	0.16	14
1259	5.07	4.21	0.17	15
1259	5.26	4.86	0.20	16

References:

Ajwa, H. (2008). Testing film permeability to fumigants under laboratory and field conditions. In *Proc Ann Int Res Conf on MeBr Alternatives and Emission Reductions* (p. 35).

Ajwa, H. and Sullivan, D.A. (2012). Soil fumigant emissions reduction using EVAL barrier resin film (VaporSafe^{TM}) and evaluation of tarping duration needed to minimize fumigant total mass loss. Study ID HA2011A submitted to DPR, 404 pp.

CIMIS (2018). California Irrigation Management Information System. California Department of Water Resources, Sacramento, CA. <http://www.cimis.water.ca.gov/WSNReportCriteria.aspx>.Dungan, R. S., and Yates, S. R. (2003). Degradation of fumigant pesticides. *Vadose Zone Journal, 2*(3), 279-286.

Gan, J., Yates, S., Ernst, F., and Jury, W. (2000). Degradation and volatilization of the fumigant chloropicrin after soil treatment. *Journal of environmental quality, 29*(5), 1391-1397.

Hilal, S., Karickhoff, S., and Carreira, L. (2003a). Prediction of chemical reactivity parameters and physical properties of organic compounds from molecular structure using SPARC. *National Exposure Research Laboratory, Office of Research and Development, US Environmental Protection Agency, Research Triangle Park, NC*.

Hilal, S., Karickhoff, S., and Carreira, L. (2003b). Verification and validation of the SPARC model. *US Environmental Protection Agency*.

Horton, R., and Chung, S. (1987). Soil heat and water flow with a partial surface mulch. *Water resources research, 23*(12), 2175-2186.

Johnson, B. and Spurlock, F. (2012). A method for estimating near-field air concentrations following tarp cutting for broadcast applications. California Department of Pesticide Regulation, Sacramento, CA. <http://www.cdpr.ca.gov /docs/emon/pubs/ehapreps/analysis_memos/2369-segawa.pdf>.

Johnson, B. and Spurlock, F. (2009). Dominant soil types associated with fumigant applications in ozone nonattainment areas. California Department of Pesticide Regulation, Sacramento, CA.

Johnson, B. (2013). Calculation of use adjustment factors for 1,3-dichloropropene with the use of totally impermeable film for broadcast shank applications. California Department of Pesticide Regulation, Sacramento, CA.

Jury, W., Spencer, W., and Farmer, W. (1983). Behavior assessment model for trace organics in soil: I. Model description 1. *Journal of environmental quality, 12*(4), 558-564.

Kandelous, M. (2018). A comparison between field estimated and HYDRUS simulated emission of 1,3-dichloropropene from agricultural field applications. California Department of Pesticide Regulation, Sacramento, CA.

Luo, Y. and Brown, C. (2018). Modeling for application factors of 1,3-dichloropropene. Sacramento, CA: California Department of Pesticide Regulation.

Majewski, M. (1995). Error evaluation of methyl bromide aerodynamic flux measurements. In Seiber, J.N, Woodrow, J.E., Yates, M.V., Knuteson, J.A., Wolfe, L.N., and Yates, S.R. (Eds.), *Fumigants: Environmental fate, exposure, and analysis.* Washington, D.C: American Chemical Society. doi: 10.1021/bk-1997-0652.ch012.

Papiernik, S. K., Yates, S. R., and Chellemi, D. O. (2011). A standardized approach for estimating the permeability of plastic films to soil fumigants under various field and environmental conditions. *Journal of environmental quality, 40*(5), 1375-1382.

Qin, R., Gao, S., Ajwa, H., Sullivan, D., Wang, D., and Hanson, B. D. (2011). Field evaluation of a new plastic film (Vapor Safe) to reduce fumigant emissions and improve distribution in soil. *Journal of environmental quality*, *40*(4), 1195-1203. doi: 10.2134/jeq2010.0443.

Schaap, M. G., Leij, F. J., van Genuchten, M. T. (2001). ROSETTA: a computer program for estimating soil hydraulic parameters with hierarchical pedotransfer functions. *Journal of hydrology, 251*(3-4), 163-176.

Šimůnek, J., Van Genuchten, M. T., and Šejna, M. (2016). Recent developments and applications of the HYDRUS computer software packages. *Vadose Zone Journal, 15*(7).

Spurlock, F., Bergin, R., Tuli, A. and Johnson, B. (2010). Fumigant transport modeling using HYDRUS 4: Development and testing of modifications to enhance fumigant field simulations. California Department of Pesticide Regulation, Sacramento, CA. <http://www.cdpr.ca.gov/docs/emon/pubs/ehapreps/analysis_memos/2221_segawa_050610.pdf>.

Spurlock, F. (2013). Effect of chloropicrin application practices on cumulative and maximum chloropicrin flux. Sacramento, CA: California Department of Pesticide Regulation.

Spurlock, F. (2014). HYDRUS estimates of cumulative 1,3-dichloropropene and chloropicrin emissions from low permeability tarp strip applications. Sacramento, CA: California Department of Pesticide Regulation.

Spurlock, F. (2015a). Variability in simulated chloropicrin and 1,3-dichloropropene volatilization from bare ground broadcast applications. Sacramento, CA: California Department of Pesticide Regulation.

Spurlock, F. (2015b). Variability in simulated chloropicrin and 1,3-dichloropropene volatilization from high density polyethylene and totally impermeable film tarped broadcast applications. Sacramento, CA: California Department of Pesticide Regulation.

Spurlock, F. (2016). Evaluation of chloropicrin buffer zone credits under California use conditions. Sacramento, CA: California Department of Pesticide Regulation.

Spurlock, F., Johnson, B., Tuli, A., Gao, S., Tao, J., Sartori, F., Qin, R., Sullivan, D., Stanghellini, M., and Ajwa, H. (2013a). Simulation of fumigant transport and volatilization from tarped broadcast applications. *Vadose Zone Journal, 12*(3).

Spurlock, F., Šimůnek, J., Johnson, B., and Tuli, A. (2013b). Sensitivity analysis of soil fumigant transport and volatilization to the atmosphere. *Vadose Zone Journal, 12*(2).

Spurlock, F., Johnson, B., and Tuli, A. (2013c). HYDRUS simulation of chloropicrin and 1,3-dichloropropene transport and volatilization in the Lost Hills fumigation trials. Sacramento, CA: California Department of Pesticide Regulation.

Tuli, A. (2011). Modeling and Monitoring Field Emissions of Fumigants Under Totally Impermeable Films (TIF). Protocol for Study 273. California Department of Pesticide Regulation, Sacramento, CA. <http://www.cdpr.ca.gov/docs/emon/pubs/protocol/study273protocol.pdf>.

Van Genuchten, M. T. (1980). A closed-form equation for predicting the hydraulic conductivity of unsaturated soils 1. *Soil science society of America journal*, *44*(5), 892-898.

Wright, D. A., Sandler, S. I., and DeVoll, D. (1992). Infinite dilution activity coefficients and solubilities of halogenated hydrocarbons in water at ambient temperatures. *Environmental science and technology, 26*(9), 1828-1831.

Yates, S. R., Gan, J., Ernst, F. F., Mutziger, A., and Yates, M. V. (1996). Methyl bromide emissions from a covered field: I. Experimental conditions and degradation in soil. *Journal of environmental quality*, *25*(1), 184-192.

APPENDIX A

Summary of HYDRUS input parameters

Table A-1. Summary of the main differences between models of each FFM code on the basis of geometry type, application depth, surface boundary conditions, tarp cut, and post-application irrigation treatments.

FFM	Geometry	Application Depth	Surface BC* 1	Surface BC 2	t @ tarp cut (days)	Other
1201	Broadcast	Shallow (30 cm)	Untarped (d = 0.5)	NA	NA	
1202	Broadcast	Shallow (30 cm)	PE tarp (d = 66)	NA	5.33	
1203	Bed	Shallow (30 cm)	PE tarp (d = 66)	Untarped (d = 0.5)	5.33	
1204	Broadcast	Shallow (30 cm)	Untarped (d = 0.5)	NA	NA	Simulated 3x post-application irrigation
1205	Bed	Shallow (30 cm)	PE tarp (d = 66)	Untarped (d = 0.5)	5.33	Simulated 3x post-application irrigation
1206	Broadcast	Deep (45 cm)	Untarped (d = 0.5)	NA	NA	
1207	Broadcast	Deep (45 cm)	PE tarp (d = 66)	NA	5.33	
1209	Bed	Drip (5 cm)	PE tarp (d = 66)	Untarped (d = 0.5)	5.5	
1210	Strip	Deep (45 cm)	Untarped (d = 0.5)	NA	NA	
1242	Broadcast	Shallow (30 cm)	TIF (d = 1326)	NA	9.33	
1243	Bed	Shallow (30 cm)	TIF (d = 1326)	Untarped (d = 0.5)	9.33	
1245	Bed	Shallow (30 cm)	TIF (d = 1326)	Untarped (d = 0.5)	9.33	Simulated 3x post-application irrigation
1247	Broadcast	Deep (45 cm)	TIF (d = 1326)	NA	9.33	
1249	Strip	Deep (45 cm)	TIF (d = 1326)	Untarped (d = 0.5)	9.33	
1259	Bed	Drip (5 cm)	TIF (d = 1326)	Untarped (d = 0.5)	9.5	

* Boundary condition at soil surface.

Table A-2. Summary of soil physical properties used in HYDRIS simulations for each soil layer (1-3). Soil cores were obtained by DPR from prepared fields prior to fumigation. BD = bulk density, theta = measured volumetric moisture content, thetaS = saturated water content, solids = solid fraction of the sample volume (1 – porosity). Ks (= saturated hydraulic conductivity), as well as alpha and n (shape parameters in the hydraulic conductivity function) are parameters fitted to measured soils data using the HYDRUS implementation of the ROSETTA pedotransfer function.

soil no.	BD1	theta1	thetaS1	BD2	theta2	thetaS2	BD3	theta3	thetaS3	solids1	solids2	solids3	alpha1	n1	Ks1	alpha2	n2	Ks2	alpha3	n3	Ks3	texture class
1	1.21	0.17	0.55	1.47	0.22	0.45	1.48	0.24	0.44	0.46	0.56	0.56	0.010	1.53	38.33	0.015	1.45	17.07	0.014	1.46	15.66	LOAM
2	1.26	0.21	0.52	1.47	0.27	0.45	1.50	0.31	0.43	0.48	0.56	0.57	0.009	1.55	28.45	0.011	1.49	13.42	0.011	1.48	8.10	LOAM
3	1.29	0.21	0.51	1.46	0.26	0.45	1.51	0.30	0.43	0.49	0.55	0.57	0.009	1.55	21.85	0.011	1.48	9.03	0.011	1.48	7.28	LOAM
4	1.27	0.07	0.52	1.26	0.14	0.53	1.41	0.18	0.47	0.48	0.47	0.53	0.014	1.41	21.66	0.016	1.39	24.86	0.015	1.38	11.27	CLAY LOAM
5	1.47	0.01	0.44	1.69	0.04	0.36	1.67	0.07	0.37	0.56	0.64	0.63	0.020	1.32	14.65	0.033	1.32	13.02	0.031	1.33	14.03	SANDY CLAY LOAM
6	1.50	0.03	0.44	1.67	0.08	0.37	1.66	0.09	0.37	0.57	0.63	0.63	0.025	1.43	34.72	0.029	1.33	12.85	0.034	1.34	18.54	SANDY LOAM
7	1.14	0.12	0.57	1.35	0.20	0.49	1.37	0.23	0.48	0.43	0.51	0.52	0.010	1.53	82.19	0.013	1.49	25.99	0.019	1.46	51.96	LOAM
8	1.29	0.15	0.51	1.38	0.12	0.48	1.47	0.16	0.44	0.49	0.52	0.56	0.012	1.47	19.55	0.010	1.53	19.28	0.011	1.47	8.57	CLAY LOAM
9	1.24	0.26	0.53	1.19	0.10	0.55	1.31	0.14	0.51	0.47	0.45	0.49	0.008	1.53	23.82	0.008	1.54	31.98	0.009	1.51	16.32	CLAY LOAM
10	1.24	0.20	0.53	1.44	0.20	0.46	1.50	0.24	0.43	0.47	0.54	0.57	0.008	1.54	24.19	0.009	1.50	7.83	0.011	1.42	5.38	CLAY LOAM
11	1.32	0.08	0.50	1.62	0.13	0.39	1.56	0.13	0.41	0.50	0.61	0.59	0.020	1.46	60.01	0.020	1.46	60.50	0.029	1.45	45.57	SANDY LOAM
12	1.39	0.14	0.48	1.35	0.18	0.49	1.51	0.41	0.43	0.52	0.51	0.57	0.013	1.37	8.89	0.012	1.39	9.74	0.007	1.53	5.64	SILTY CLAY
13	1.28	0.10	0.52	1.40	0.14	0.47	1.55	0.21	0.41	0.48	0.53	0.59	0.024	1.46	83.25	0.019	1.45	32.09	0.025	1.39	21.07	SANDY LOAM
14	1.37	0.12	0.49	1.39	0.21	0.48	1.42	0.29	0.46	0.52	0.52	0.54	0.009	1.51	11.69	0.008	1.55	11.02	0.009	1.49	8.20	CLAY LOAM
15	1.30	0.13	0.51	1.25	0.18	0.53	1.45	0.26	0.45	0.49	0.47	0.55	0.009	1.54	19.69	0.008	1.54	23.70	0.010	1.50	9.58	LOAM
16	1.09	0.18	0.59	1.13	0.22	0.58	1.26	0.23	0.53	0.41	0.42	0.47	0.019	1.34	59.56	0.018	1.34	46.55	0.016	1.38	25.80	CLAY

Table A-3. Principal input variables required for HYDRUS simulations and their data source.

Input variable (units)	Variable name	Source
ρ_b	soil bulk density[A]	Measured
θ_s (-)	saturated water content[A]	Calculated from bulk density ($\theta_s = 1 - \rho_b/2.65$)
θ_i (-)	initial water content[A]	Measured
θ_r (-)	residual water content[A]	Assumed = 0
α (cm^{-1})	VG retention model parameter[B]	Calculated independently for each layer of the soil profile from measured ρ_b and sand, silt, and clay content using HYDRUS' implementation of ROSETTA soil pedotransfer functions
n (-)	VG retention model parameter[B]	
K_s (cm d^{-1})	saturated hydraulic conductivity	
C_n (J cm^3 K^{-1})	volumetric solid phase heat capacity[A]	HYDRUS default
λ_L, b_1, b_2, b_3	soil thermal conductivity parameters[A]	HYDRUS default for sand, loam, or clay soil (from Horton and Chung, 1987) and applied in accordance to 'coarse', 'moderately coarse/medium textured', and 'fine textured' soil texture categories, respectively, as described in Table 2.
$T_0(t)$ (C)	soil surface temperature as a function of time *t*	Bare, PE: sine-wave estimation scheme (Spurlock 2013) based on September temperature conditions in Fresno County. TIF: measured (Lost Hills study)
D_g (cm^2 d^{-1})	gas phase diffusion coefficient	SPARC on-line calculator (Hilal et al., 2003a, 2003b)
D_gE_a (J mol^{-1})	D_g activation energy[C]	
D_w (cm^2 d^{-1})	aqueous phase diffusion coefficient	
D_wE_a (J mol^{-1})	D_w activation energy[C]	
K_h (-)	Henry's law constant	1,3-D: Wright (1992)
K_hE_a (-)	K_h activation energy[C]	
k_1 (d^{-1})	first-order degradation rate constant[A]	Calibrated in Lost Hills study field 1, Spurlock et al. (2013a)
k_1E_a (J mol^{-1})	k_1 activation energy[A,C]	Mean data of Dungan and Yates (2003) and Gan et al. (2000)
OC (g_{OC} g_{soil}^{-1})	soil organic carbon mass fraction[A]	Lost Hills study mean of 3 fields, Spurlock et al. (2013a)
K_d (cm^3 g^{-1})	soil partition coefficient[A]	Calculated from calibrated K_{OC} and measured OC ($K_d = K_{OC} * OC$), from Spurlock et al. (2013a).

d (cm)	tarp boundary layer depth[D]	Bareground value: Jury et al. (1983) PE value: calculated from values in Paperniek et al. (2011), via Spurlock (2015) TIF value: calibrated value from the Lost Hills study, Spurlock et al. (2013a)
λ_w (cm)	longitudinal dispersivity	HYDRUS default

[A] required for each soil layer. [B] van Genuchten (VG) soil-water retention model was used (van Genuchten, 1980). [C] activation energies describe the temperature dependence of the associated parameter. [D] tarp boundary layer depth describes tarp permeability, assumed independent of temperature – see calibration results of Spurlock et al. (2013a)

Table A-4. Chemical property input variables used for HYDRUS simulations.

Input Variable (units)	Variable name	1,3-D value
D_g (cm^2 d^{-1})	Gas diffusion coefficient	6886
D_gE_a (J mol^{-1})	D_g activation energy	4560
D_w (cm^2 d^{-1})	Aqueous diffusion coefficient	0.735
D_wE_a (J mol^{-1})	D_w activation energy	18035
K_H (-)	Henry's constant	0.05
K_HE_a (J mol^{-1})	K_H activation energy	32085
k_1 (d^{-1})	Degradation constant	0.0965
k_1E_a (J mol^{-1})	k_1 activation energy	59028
K_{OC} (ml [g OC]$^{-1}$)	OC-normalized soil partition coefficient	28
d (cm)	Boundary layer depth (tarp permeability)	bareground: 0.5 PE: 66 TIF: 1326

APPENDIX B

Example input files

Annotated example: Main HYDRUS input file for FFM 1201 (SELECTOR.in). The "# xxxxx #" entries are placeholders for measured soil core data used in each simulation. Initial water contents are input in DOMAIN.in input file for soil layers 1-3. Simulations of each FFM vary primarily in terms of geometry, stagnant boundary layer depth, and tarp removal time.

```
ptf #
Pcp_File_Version=4
*** BLOCK A: BASIC INFORMATION ****************************************
Heading
Welcome to HYDRUS
LUnit  TUnit  MUnit  (indicated units are obligatory for all input data)
cm
days
ug
Kat (0:horizontal plane, 1:axisymmetric vertical flow, 2:vertical plane)
 2
MaxIt   TolTh   TolH InitH/W  (max. number of iterations and tolerances)
 10    0.001     1     t
lWat lChem lSink Short Inter lScrn AtmIn lTemp lWTDep lEquil lExtGen lInv
 t    t    f    t    f  t    t    t    f     t     t     f
lUnsatCh lCFSTr   lHP2   m_lActRSU lDummy  lDummy  lDummy
 f      f      f      f      f      f      f
 PrintStep  PrintInterval lEnter
       1           0      f
*** BLOCK B: MATERIAL INFORMATION *************************************
NMat    NLay    hTab1   hTabN     NAniz
 3      1    0.0001   10000
   Model   Hysteresis
    0        0
 thr    ths   Alfa     n       Ks     l
 0.0 # thetaS1 # # alpha1  # #   n1    # #   Ks1   #    0.5
 0.0 # thetaS2 # # alpha2  # #   n2    # #   Ks2   #    0.5
 0.0 # thetaS3 # # alpha3  # #   n3    # #   Ks3   #    0.5
*** BLOCK C: TIME INFORMATION *****************************************
      dt      dtMin      dtMax     DMul    DMul2  ItMin ItMax  MPL
```

Soil hydraulic properties: 3 soil layers at 0-10 cm, 10-30 cm, and 30-120 cm. ThetaS1-3 are laboratory-measured values; alfa, n, Ks are estimated based on measured soil texture in the HYDRUS implementation of the ROSETTA pedotransfer function.

```
    0.0001     1e-007      0.1     1.3     0.7     3     7    500
     tInit       tMax
      0.33       21.33
TPrint(1),TPrint(2),...,TPrint(MPL)
    0.3717     0.4134     0.4551     0.4968     0.5385     0.5802
…
   21.1383      21.33
*** BLOCK D: SOLUTE TRANSPORT INFORMATION **************************************************
 Epsi  lUpW  lArtD lTDep    cTolA    cTolR   MaxItC    PeCr  Nu.ofSolutes Tortuosity Bacter Filtration
  0.5    f    f    t        0        0    1       2       1        t        f        f
  lWatDep    lInitM   lInitEq   lTortM   lFumigant lDummy   lDummy   lDummy   lDummy   lDummy   lDummy
       f        t        f        t        t        f        f        f        f        f        f
    Bulk.d.     DisperL.      DisperT     Frac     ThImob (1..NMat)
     #  BD1   #         13          3          1          0
     #  BD2   #         13          3          1          0
     #  BD3   #         13          3          1          0
       DifW       DifG             n-th solute
     0.735       6886
       Ks         Nu        Beta       Henry      SnkL1      SnkS1      SnkG1     SnkL1'     SnkS1'     SnkG1'     SnkL0      SnkS0      SnkG0       Alfa
     0.154          0          1       0.05     0.0965     0.0965     0.0965          0          0          0          0          0          0          0
     0.044          0          1       0.05     0.0965     0.0965     0.0965          0          0          0          0          0          0          0
         0          0          1       0.05     0.0965     0.0965     0.0965          0          0          0          0          0          0          0
Temperature Dependence
       DifW       DifG             n-th solute
     18035       4560
       Ks         Nu        Beta       Henry      SnkL1      SnkS1      SnkG1     SnkL1'     SnkS1'     SnkG1'     SnkL0      SnkS0      SnkG0       Alfa
         0          0          0       32085      59028      59028      59028          0          0          0          0          0          0          0
     cTop       cBot
         0          0          0          0          0          0          0          0        0.5
     tPulse
       100
  AddFumigant
       f
*** BLOCK E: HEAT TRANSPORT INFORMATION ****************************************************
```

tInit = beginning of application = 0.33 days
tMax = simulation end = 21.33 days

Print times (cut for brevity) cover every hour of the simulation run between tInit and tMax.

Tortuosity = Moldrup model

BDx = bulk density for layer "x". Ks = linear distribution coefficient calculated from Lost Hills calibrated 1,3-D K_{OC} and OC contents (Spurlock et al. 2013a).

SnkL1/S1/G1 = bulk degradation rate constants and activation energies = calibrated from Lost Hills study for 1,3-D.

d = stagnant boundary layer depth, bare = 0.5, PE tarp = 66, TIF = 1326. tPulse = time of tarp removal (days) = 100 for untarped (no removal), 5.33 for PE tarp, 9.33 for TIF tarp.

```
   Qn      Qo        Disper.       B1         B2         B3         Cn         Co         Cw
 #  solids1  #      0 .011     5      1 #   b1   # #   b2   # #   b3   #1.43327e+014 1.8737e+014 3.12035e+014
 #   solids2   #     0.0032      5      1 #   b1   # #   b2   # #   b3   # 1.43327e+014 1.8737e+014 3.12035e+014
 #    solids3  #      0      5      1 #   b1   # #   b2   # #   b3   #1.43327e+014 1.8737e+014 3.12035e+014
     TTop       TBot
       0         0         0         0         0         0
    tAmpl     tPeriod
       0         1
*** END OF INPUT FILE 'SELECTOR.IN' ************************************
```

Solids "x" = volume fraction solids in layer "x". Calculated as 1-thetaS"x". Heat transport parameters = default for Loam soils.